MERGERS AND STARBURSTS AT LARGE REDSHIFTS: THE CASE OF 3C 368[a]

S. DJORGOVSKI[b),c),d)]
Harvard-Smithsonian Center for Astrophysics, 60 Garden Street, Cambridge, Massachusetts 02138

H. SPINRAD[b)]
Astronomy Department, University of California, Berkeley, California 94720

J. PEDELTY AND L. RUDNICK
Department of Astronomy, University of Minnesota, Minneapolis, Minnesota 55455

A. STOCKTON[c)]
Institute for Astronomy, University of Hawaii, Honolulu, Hawaii 96822
Received 24 December 1986; revised 20 February 1987

ABSTRACT

We report the results of a multiwavelength study of the high-redshift radio galaxy 3C 368, which is observed at a lookback time of about two-thirds of the present galaxian age. This galaxy has optical and spectroscopic properties that are perhaps typical for the powerful 3CR galaxies at large redshifts ($z > 1$), though it is probably more luminous than the most, both in continuum and [O II]. Its resolved, multicomponent morphology of the starlight continuum and the [O II] λ 3727 emission-line gas, and the properties of the ionized-gas velocity field, are suggestive of a strong and highly dissipative merger. There is a good positional and morphological coincidence between the line emission and the optical continuum. The proposed merger is probably enhancing the star formation over the whole galaxy (as evidenced by the large luminosity and the blue colors of the optical continuum), and may be the primary source of the fuel for, or even the trigger of, the strong radio emission from the system. The morphological and spectroscopic similarities with other 3CR galaxies at $z > 1$ suggest that spectacular merging was a common process in such systems at early epochs. The mergers may be identified with the process of transformation of (large?) E galaxies into cD's, and the epoch of such "secondary" formation of gE/cD galaxies may be signalled by the appearance of powerful radio sources at $z \sim 1$–2. The galaxy evolution models with a continuing star formation, suggested by the colors and magnitudes of high-redshift 3CR galaxies, may be understood in terms of a declining sequence of starbursts, stimulated by gas-rich mergers. There are also some indications of an ongoing interaction between the radio lobes and the ambient gas: both radio lobes show a prominent Faraday rotation and depolarization, probably caused by the intervening plasma along the line of sight. There is also a reasonable positional coincidence between the southern radio lobe and the emission-line gas. However, the evidence for an interaction between the radio plasma and the gas in the host galaxy is neither clear nor unambiguous.

I. INTRODUCTION

In 1951 or so, Baade and Minkowski identified the second-brightest radio source in the sky, Ryle 19.01 = Mills 19 + 4, also known as Cygnus A, with a peculiar extragalactic nebula, "... a very curious object which seems to defy classification" (Baade and Minkowski 1954a). However, the photographic images and spectra of this object that they obtained led them to conclude that the source represents two galaxies in a collision, at a then high redshift of 0.0561. They went on to speculate that many of the radio sources unidentified at the time may be more distant examples of this phenomenon (Baade and Minkowski 1954b).

Their prediction has been correct: to this day, powerful radio galaxies remain among the deepest and most useful probes of the universe at cosmological redshifts, now reaching up to $z \simeq 1.8$ (Spinrad and Djorgovski 1984b; Spinrad 1985; Djorgovski 1987). The sample of 3CR galaxies, which also includes Cyg A as 3C 405, has now been almost completely identified (cf. Spinrad *et al.* 1985), which is still a unique distinction for a deep extragalactic sample, and makes many interesting tests possible. This sample provided us with strong evidence for galaxy evolution at lookback times exceeding half of the Hubble time (Lilly and Longair 1984; Djorgovski, Spinrad, and Marr 1985; Djorgovski, Spinrad, and Dickinson 1987), and may even be usable for a measurement of the q_0 parameter at infrared wavelengths (Spinrad and Djorgovski 1987). The 3CR galaxies are generally identifiable with giant ellipticals and brightest cluster members, as far as we can tell (up to $z \sim 0.7$, or so), and they do not differ systematically from brightest cluster members in their near-IR properties at any redshift where direct comparisons are possible (Lebofsky and Eisenhardt 1986). However, they are often somewhat unusual in their appearance, even at the low redshifts: many 3CR galaxies have dust patches or features suggestive of tidal interactions; some are multiple-nuclei cD's or distorted doubles. On the other end of the distance scale, the shapes of 3CR galaxies at large redshifts are often very elongated, and even multimodal; in

[a)] Based in part on the observations done at Lick Observatory, University of California.
[b)] Visiting Astronomer, Kitt Peak National Observatory, National Optical Astronomy Observatories, operated by AURA, Inc., under contract with the NSF.
[c)] Visiting Astronomer, Canada-France-Hawaii Telescope, operated by the National Research Council of Canada, the Centre National de Recherche Scientifique de France, and the University of Hawaii.
[d)] Harvard Junior Fellow.

 0004-6256/87/061307-11$00.90

all such cases observed to date with long-slit spectrographs, there is a strong [O II] λ 3727 emission, resolved and mostly coincident with the galaxy continuum, and with a large velocity field (Spinrad and Djorgovski 1984a,b). Understanding the physical processes behind such phenomena is essential if we are to use the powerful radio galaxies as a cosmological tool with some confidence. One of the best and most spectacular is 3C 368, a radio galaxy at $z = 1.132$, and we have chosen it as a good case for a detailed study.

II. THE DATA

We obtained direct *BVR* images of 3C 368 on the night of 15 May 1986 UT, with a RCA 320×512 CCD and the FOCAS system at the Cassegrain focus of the Canada-France-Hawaii (CFH) 3.6 m telescope at Mauna Kea, under photometric conditions and half-arcsec seeing, with a sampling of 0.22 arcsec/pixel. Three exposures of 600 s each were obtained, one in each of the three bands. The M92 standard field (Christian *et al.* 1985) was used for the photometric calibration. A section of the stacked image is shown in Fig. 1. The photometry gives for the whole galaxy:

$$V = 21.3 \pm 0.1\,,$$
$$(B - V) = 0.05 \pm 0.15\,,$$
$$(V - R) = 0.70 \pm 0.15\,.$$

These values were corrected for the Galactic extinction, by assuming $E_{B-V} = 0.16$ (Burstein and Heiles 1982), and for the contributions of the strong emission lines (typically a few percent), as derived from our slit spectroscopy. Both the apparent magnitude and the blue colors are typical for the $z > 1$, 3CR galaxies (Djorgovski, Spinrad, and Dickinson 1987).

Since our earlier spectroscopy indicated that the galaxy has strong and extended [O II] emission, we obtained an image in a narrow bandpass (FWHM = 36 Å), centered on the redshifted [O II] λ 3727 line, on the night of 16 October 1985 UT, using a TI three-phase 500×500 CCD in the *Galileo*/IfA camera, at the Cassegrain focus of the CFH telescope. The scale with a focal reducer was 0.3 arcsec/pixel. One 1800 s integration was obtained in FWHM $\simeq$ 0.8 arcsec seeing. This image is shown in Fig. 2. It is evident that the line emission follows the continuum, both in the shape and extent, although the relative intensity may vary along the galaxy. The important point here is that the bulk of the line emission has clearly a nonnuclear origin, and that outside the nuclear region the emission-line gas is distributed roughly in the same way as the stars. Similar results were obtained independently by Schild and Eisenhardt (1986, private communication).

Slit spectra of the galaxy were obtained on several occasions. On the night of 28 July 1984 UT, we obtained two exposures of 2000 and 3600 s, using the Miller-Robinson-Stover Cassegrain CCD spectrograph at the Lick 3 m telescope. The spectra were taken with the slit P.A. = 10° (along the galaxy's major axis), and flux calibrated with the spectra of the standard star Hiltner 102 (Stone 1977). Two more exposures of 3000 s each were obtained on the following night, with the slit P.A. = 90°, centered on two different positions (continuum condensations). This procedure enabled us to do a rough [O II] emission mapping of the galaxy, as illustrated in Fig. 3. Evidently, the velocity field varies with the location and direction, and has the largest extent along the major axis of the system. Two more exposures were obtained with the Cryocam spectrograph at the Kitt Peak 4 m telescope, of 3000 s each, both with the slit P.A. = 10°: one on the night of 17 April 1985 UT, calibrated with the standard star Kopff 27, and one on the night of 12 May 1986 UT,

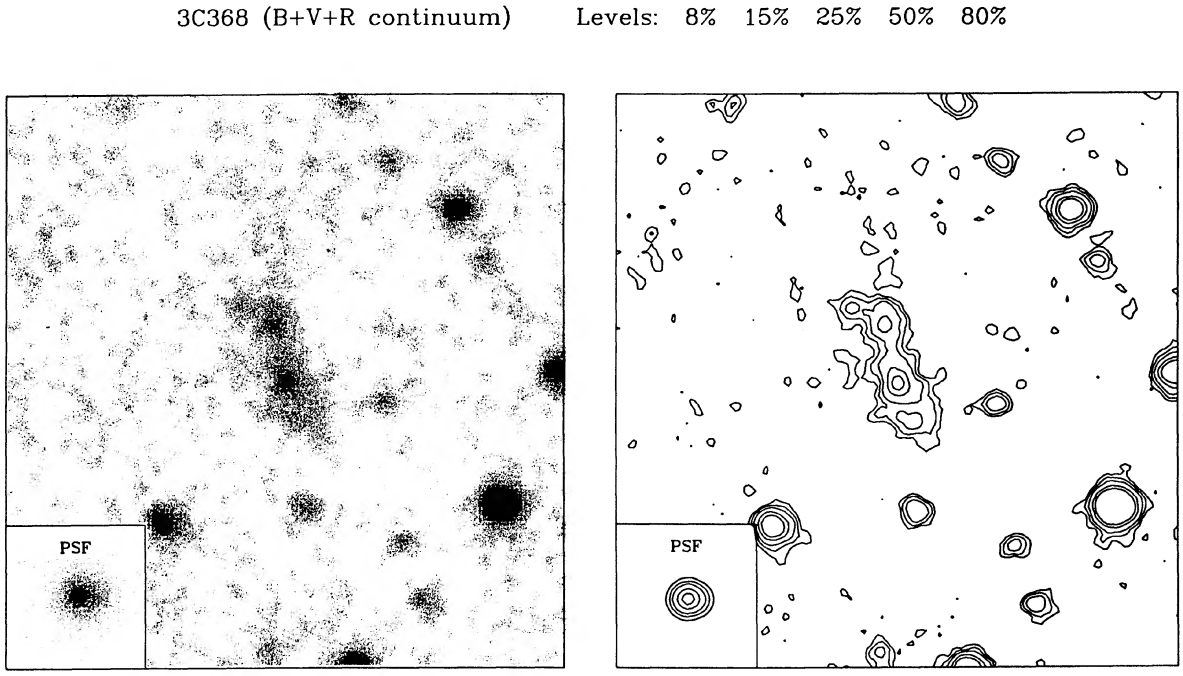

FIG. 1. A stack of the continuum (*BVR*) images of 3C 368, obtained at CFHT. The field shown is 27.6 arcsec square, with N to the top, E to the left. The contour levels are at 8%, 15%, 25%, 50%, and 80% of the intensity peak of the radio galaxy.

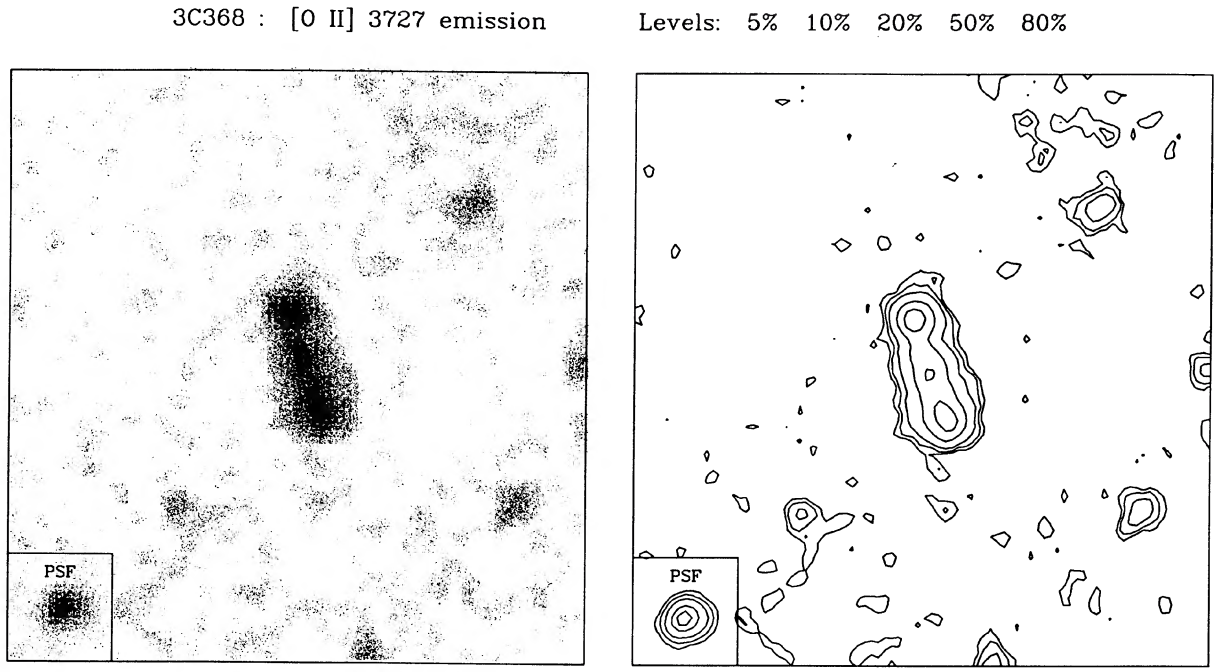

FIG. 2. Image of 3C 368 obtained with an interference filter centered on the redshifted [O II] λ 3727 line. The field size and orientation are as in Fig. 1. Note the excellent correspondence in shape and orientation between the continuum and line emission. The contour levels are at 5%, 10%, 20%, 50%, and 80% of the peak intensity of the radio galaxy.

calibrated with the standard star BD +25°3941 (Stone 1977). The expanded region around the [O II] line from the later exposure is shown in Fig. 4. The extracted spectra, combined from the two Kitt Peak exposures, are shown in Fig. 5. Table I shows the measurements of strong emission lines. The overall ionization is fairly low.

The imaging nature of CCD spectrographs enables us to do spatial mapping of the extended line emission, at different locations along the slit. The results are shown in Fig. 6, for both [O II] λ 3727 and [Ne III] λ 3869 lines (the other lines were too weak to analyze in this way). It can be seen that the equivalent width (essentially, the ratio line/continuum) is largest in the regions *between* the continuum condensations. Note that both the velocity gradient and the linewidth are stronger at the northern side of the system.

To learn more about the radio source and its possible relationship to the optical continuum and emission-line gas, we obtained radio continuum observations of 3C 368 with the NRAO Very Large Array (VLA).* Observations at 20 cm wavelength were made on 20 February 1985 UT, while the array was in its standard A configuration. Two sets of receivers with center frequencies of 1502.4 and 1452.4 MHz and with 25 MHz bandwidths were used. The galaxy was also observed at 6 cm wavelength in the standard B configuration on 1 June 1985 UT. The center frequencies were 4885.1 and 4835.1 MHz, and the bandwidths were 50 MHz. In each session, the source was observed for a total of six 18 min scans at a variety of hour angles. These data were calibrated using the standard NRAO software, and were used to produce total intensity and polarization maps with identical resolutions of 1.8×1.3 arcsec in P.A. = 57°. Higher-resolution radio observations were obtained at 6 cm wavelength on 19 March 1986 UT. The array was again in its standard A configuration. The center frequencies and bandwidths were the same as used in the previous 6 cm observations, but only a single 10 min snapshot was obtained while the source was near transit. The maps produced from these data had a resolution of 0.35 arcsec.

The radio structure of 3C 368 with 0.35 arcsec resolution is shown in Fig. 7. The structure is typical of high luminosity radio sources, with intense hotspots and diffuse emission trailing toward the weak nuclear core. This structure is designated Type II by Fanaroff and Riley (1974). Note the marginal detection ($\simeq$0.45 mJy, or 2×10^{24} W Hz^{-1} at 5 GHz) of a radio core. The significance of this detection is formally 4 σ, based on the rms noise in a region of the map removed from the source. The cross marks the position of 3C 368 as determined by Gunn *et al.* (1981), with the size of the cross equal to their overall error of 0.4 arcsec. Note the low fractional polarization of the diffuse emission in the southern lobe. The 6 and 20 cm equal-resolution radio observations allow us to measure the polarization and spectral-index properties of 3C 368. Maps were produced at both frequencies within the 20 cm band, separated by 50 MHz, and gave us a total of three points to use for Faraday rotation measurements. The distribution of depolarization (defined as percent polarization at 20 cm divided by that at 6 cm) and Faraday rotation are shown in Fig. 8. The spectral indices at the peaks in both the north and the south hotspots are $\alpha = -1.3$, where $S_\nu \sim \nu^\alpha$.

The radio observations of 3C 368 can be used to derive estimates of the radio-source physical properties. The total radio luminosity is $\sim 10^{45}$ erg s^{-1}, derived using a spectral index of -1.1 between 10^7 and 10^9 Hz, which steepens to -1.3 from 2×10^9 to 10^{11} Hz (cf. Kellermann *et al.* 1969). This luminosity is comparable to that of Cyg A (Perley *et al.*

*The VLA is a facility of the National Radio Astronomy Observatory, operated by Associated Universities, Inc., under contract with the National Science Foundation.

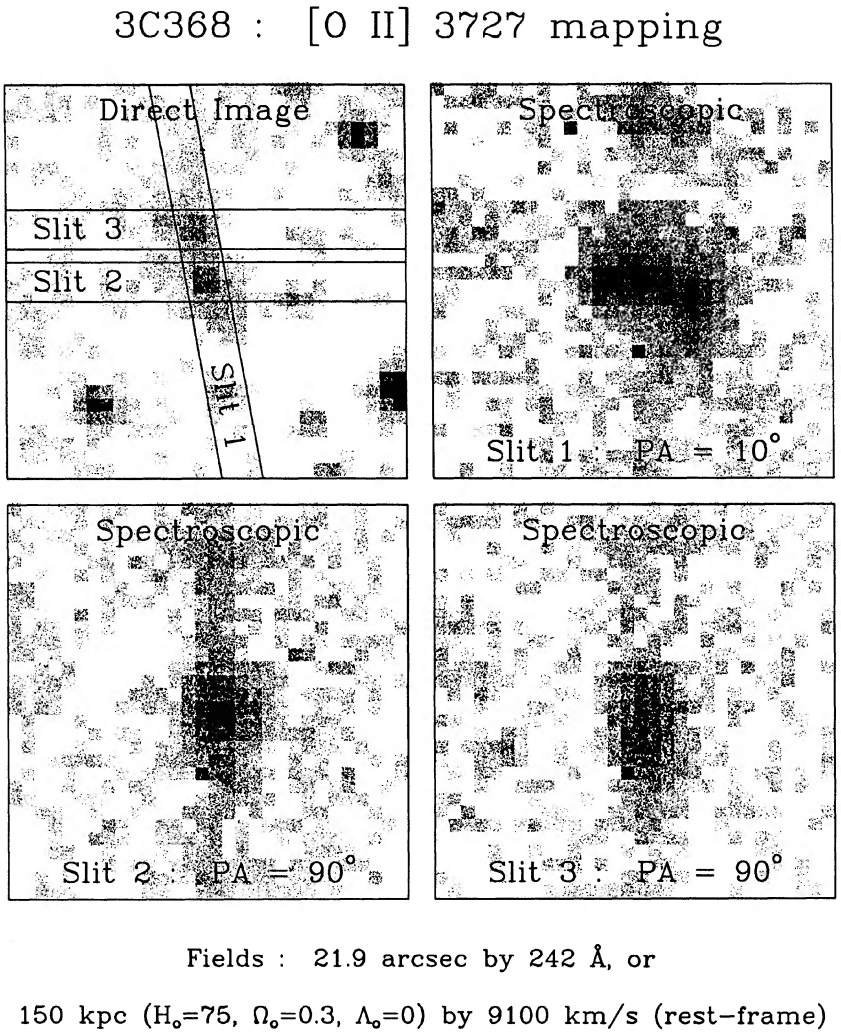

FIG. 3. Long-slit mapping of the [O II] λ 3727 emission. The top left-hand panel shows the continuum image (as in Fig. 1), with three spectroscopic slit positions drawn. The remaining three panels show enlarged portions of the sky-subtracted spectroscopic CCD frames obtained at Lick, centered on the [O II] line. On all three spectroscopic frames, the spatial dimension (along the slit) runs left to right, and the wavelength, or velocity, dimension runs from top to bottom. Note that the velocity structure is different at different positions in the galaxy.

1984), and is an order of magnitude greater than the total emission-line luminosity. The spectral indices of 3C 368 are at the steep extreme of the distribution of 3C sources (Kellermann *et al.* 1969), but show only mild curvature from 38 MHz to 5 GHz. The steep spectra are therefore not likely to arise from synchrotron energy losses, and their origin is presently unclear.

We use the minimum-pressure analysis of Burns, Owen, and Rudnick (1979) to derive the total energy in relativistic particles and magnetic fields, and the strength of the magnetic field. In 3C 368, this total energy is $\sim 5\times 10^{58}$ erg, and the magnetic field strength is ~ 300 μG. The single-dish measurements of Kellermann *et al.* (1969) indicate that the high-resolution VLA observations are not missing significant amounts of flux ($\leqslant 10\%$). If, however, 10% of the flux was distributed uniformly throughout the source, the total energy would be approximately doubled.

To interpret these data in terms of physical scales, we must choose a cosmological model. In a Friedman model with $H_0 = 75$ km s^{-1} Mpc^{-1}, $q_0 = 0.2$, and $\Lambda_0 = 0$, at $z = 1.132$, 1 arcsec corresponds to 6.62 kpc, and the distance modulus is $(m - M) = 43.97$, corresponding to the luminosity distance of $\simeq 1.92\times 10^{28}$ cm. If galaxies formed at $z_{gf} = 5$, then the age of 3C 368 as observed is 2.85 Gyr in this cosmology, or 30.7% of the present galaxian age; if galaxies formed at $z_{gf} = 10$, these numbers are 3.36 Gyr, and 34.4%, respectively. In any case, we see 3C 368 as a relatively young galaxy.

III. 3C 368 AS A DISSIPATIVE MERGER

The multicomponent morphology (multimodal shape) of 3C 368 and the associated [O II] velocity field are suggestive of a spectacular merger of gas-rich galaxies at a large redshift. This hypothesis is supported by the good correspondence of emission-line gas and the features in the velocity field with the continuum condensations. The velocity gradient and the linewidth can be interpreted as the shear and the turbulence of the velocity field. The streaming velocities observed in the ionized gas (several hundred km s^{-1}) are typical of the velocity dispersions in moderately rich galaxy clusters. There are many faint galaxies in the field, but we do not yet have redshift measurements for any of them, and thus we cannot at this point claim detection of a cluster around 3C 368.

The observed line energy of [O II] λ 3727 is $\simeq 8.2\times 10^{-15}$

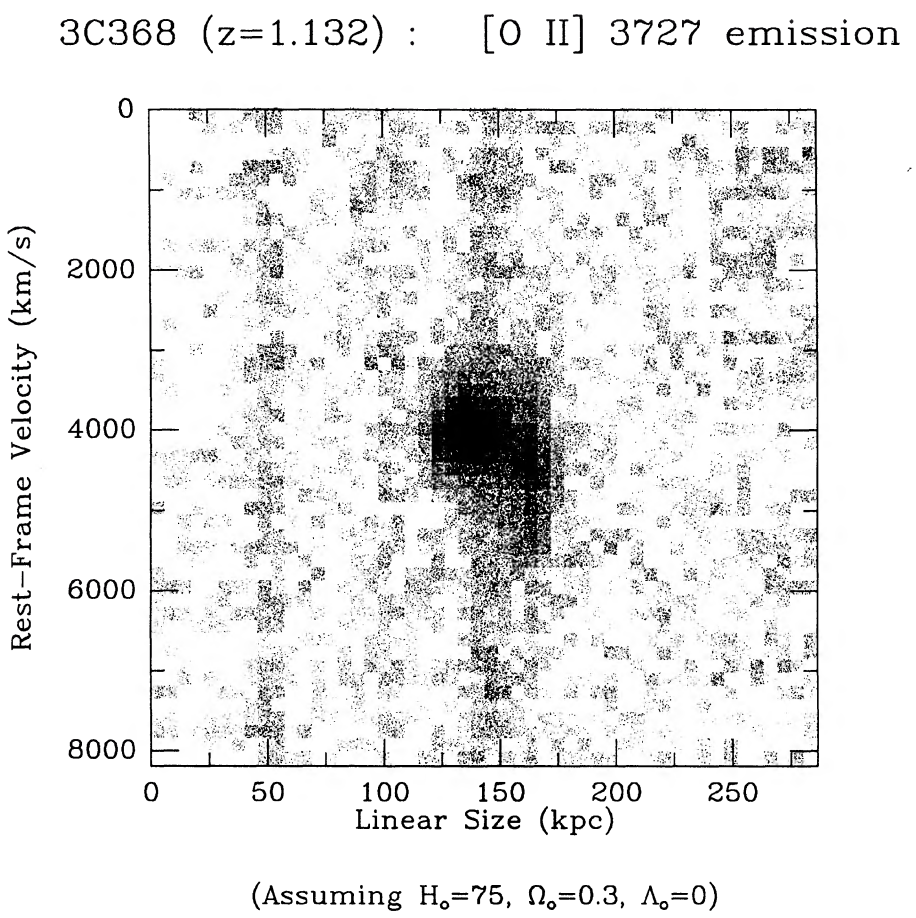

FIG. 4. "Phase-space" diagram of the [O II] emission-line gas along the galaxy's major axis. This is an enlarged portion of a spectroscopic CCD frame obtained at Kitt Peak, corresponding roughly to the top right-hand panel of Fig. 3. The physical scale in kpc was computed by assuming a Friedman cosmology with $H_0 = 75$, $\Omega_0 = 0.3$, and $\Lambda_0 = 0$.

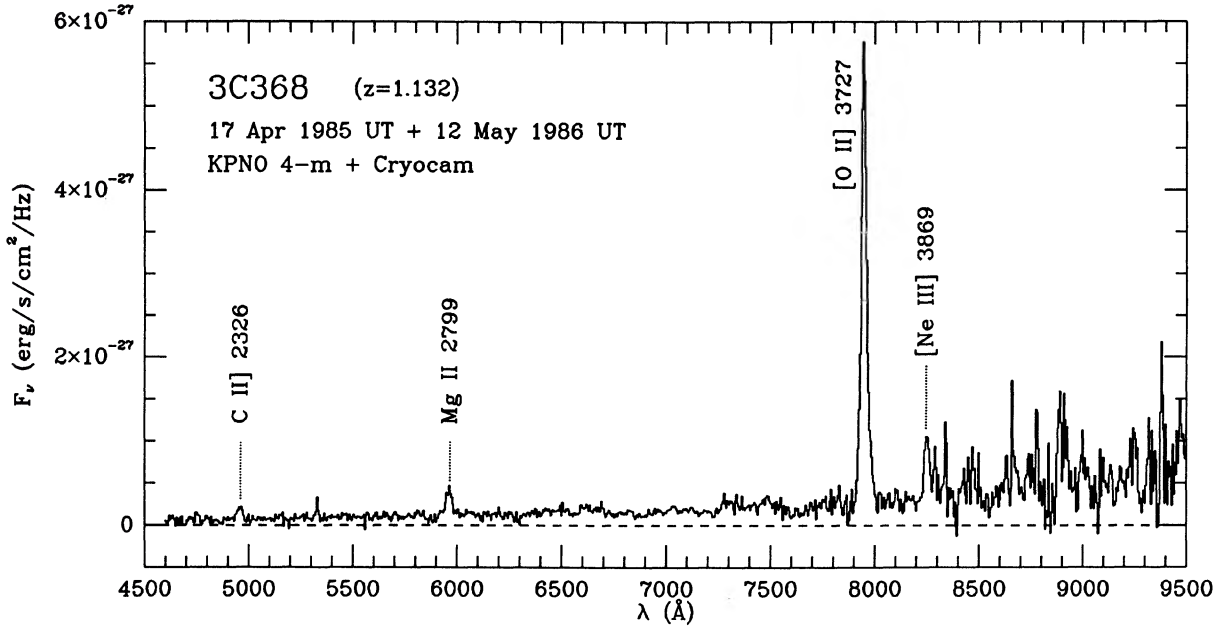

FIG. 5. Combined visual/near-IR spectrum of 3C 368, obtained at Kitt Peak. Note the enormously strong [O II] line, and the complete absence of high-ionization lines. This spectrum is relatively typical for $z > 1$, 3CR galaxies.

TABLE I. Emission lines in 3C 368.

Line	λ obs.	W_λ (Å)	Relative int.
C II 2326	4960.0	70	0.082
Mg II 2799	5960.6	102	0.135
O II 3727	7946.7	646	1
Ne [III] 3869	8251.2	51	0.097

erg cm^{-2} s^{-1} (this may be a slight underestimate, because not all of the light goes through the spectrograph slit). In the cosmological model described above, this corresponds to the large rest-frame line luminosity in excess of 3.8×10^{43} erg s^{-1}, or $10^{10}L_\odot$. The [O II] line can be either collisionally or radiatively excited, and we must explain where its $>7\times10^{54}$ photons s^{-1} come from.

The galaxy does not possess a visible bright active nucleus, which would provide a sufficient photoionization to support this strong emission. However, star formation at the scales observed may make a substantial contribution of ionizing radiation. The magnitudes and colors of 3C 368 are not too different from other 3CR galaxies at similar redshift, and the sample as a whole favors the active-star-formation models by Bruzual (1981, 1983). The model that best describes the data is a so-called $\mu = 0.5$ model, in which the star-formation rate declines exponentially with the e-folding time of about 1.4 Gyr. We can use the synthesized spectral-energy distribution of such a model, scaled so that it matches the observed magnitude of the galaxy, and compute how many ionizing photons are produced. To do so, we computed the models with two different IMFs, Salpeter and Miller-Scalo (they differ in shape at the massive end, which contributes most of the ionizing photons), and assumed the same cosmology as mentioned above. The Salpeter IMF model produces $\sim2.0\times10^{55}$ ionizing photons s^{-1}, and the Miller-Scalo IMF model $\sim1.8\times10^{54}$ ionizing photons s^{-1}. This is probably a realistic range, but it is possible, although perhaps unlikely, that an IMF with a much higher proportion of blue giants operates in 3C 368. If a less strongly evolving $\mu = 0.7$ model (e-folding time of ~0.8 Gyr) is used, and scaled in the same way, these numbers are lowered by only $\sim10\%$. If we can assume that the radiation transfer in the environment of 3C 368 is not too different from a giant extragalactic H II region, there should be about ten ionizing photons for every [O II] λ 3727 photon produced. Thus, the photoionization by the young stars is insufficient to maintain the strong [O II] emission in 3C 368, and in the absence of a detectable active nucleus, the bulk of the line emission then must be collisionally excited. The presence of any internal extinction (e.g., dust) would aggravate the photoionization problem further. It is interesting to note that in all of the evolution models mentioned above, the predicted Type II supernova rate is about 25–30 per century, in the Earth's observer frame. These supernovae may contribute significantly to the energetics of the emission-line gas, and thus alleviate the ionization-energy requirements stated above.

We next need to ask what is the available kinetic energy from such a hypothetical collision. From the range of population-synthesis models and our photometry, and our chosen cosmology, we infer that the *baryonic* mass of 3C 368 is in the range of $(2–10)\times10^{11}\ M_\odot$. For typical collisional velocity of 400 km s^{-1} in the rest frame, as observed, that corresponds to a kinetic energy in the range of $(3–15)\times10^{59}$ erg,

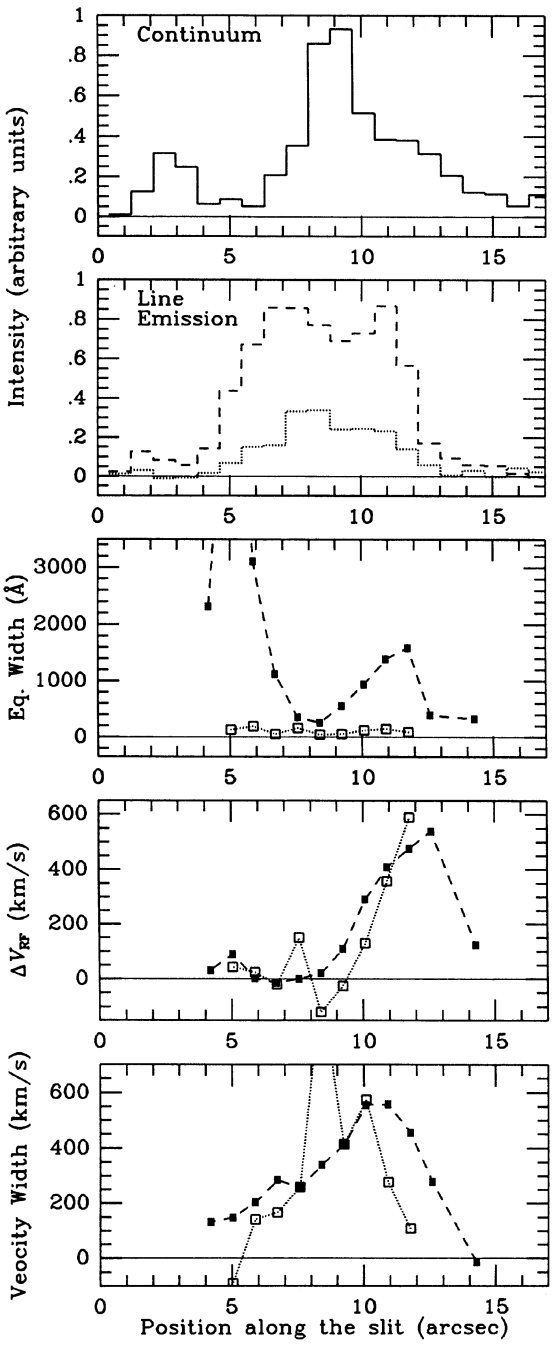

FIG. 6. Analysis of the spatially resolved line emission in [O II] λ 3727 (solid squares, dashed line), and Ne III] λ 3869 lines (light squares, dotted line). The points correspond to the individual CCD columns (1-pixel-wide spectra) on the spectroscopic image partly shown in Fig. 4. North is to the right. The kinematics of the gas is very similar in the two emission lines, although the [O II] is much stronger. The velocity width (bottom panel) has been corrected for the instrumental resolution.

for the *baryonic* mass only. We must recall that the original collisional velocity could have been somewhat higher, since some energy must have already dissipated, and that there can be an unknown amount of dark material, which can push the kinetic energy estimates up by an order of magni-

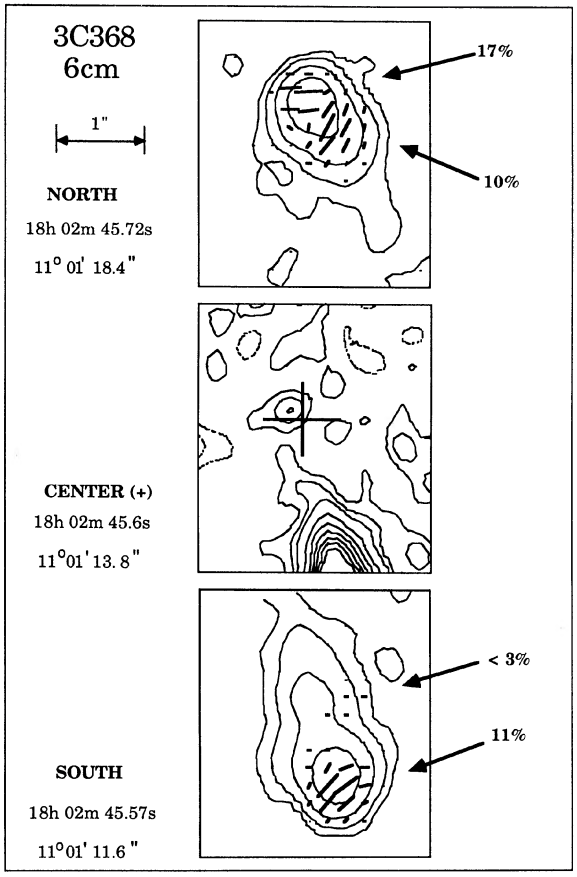

FIG. 7. VLA maps showing the total intensity, polarized emission, and polarization angle for 3C 368 at a wavelength of 6 cm. The beam size is 0.36×0.34 arcsec, at a position angle of 9°. Positions are listed for the centers of the north and south lobe boxes, and for the cross (+) showing the position of the optical ID in the central box. Contour levels are: in the central box, (− 2, − 1, 1, 2, 3, 4, 5, 6, 7, 8, 9)×0.14 mJy/beam, in the north and south lobe boxes, (1, 4, 16, 64)×0.25 mJy/beam. A vector length of 1 arcsec represents 11 mJy of polarized flux. Fractional polarization values are indicated for the two polarized emission peaks in the north lobe, and for one in the south. A 3σ limit is also quoted for the secondary total-intensity peak in the south.

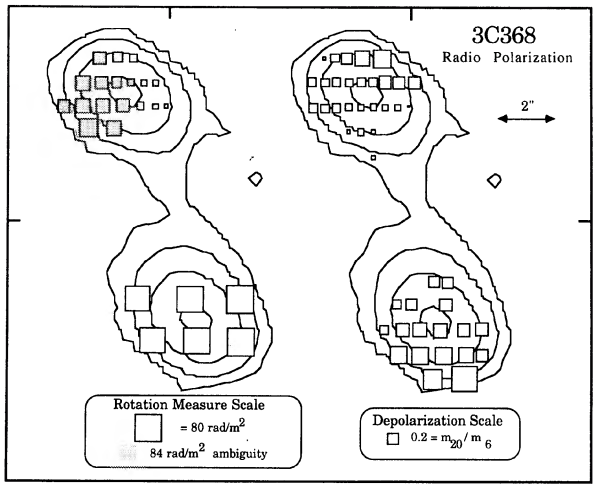

FIG. 8. Contour maps of 3C 368 at 6 cm wavelength, with a beam size of 1.8×1.3 arcsec, at a position angle of 57°. Contour levels are (1, 6, 36, 216)×0.3 mJy/beam. Other symbols show the depolarization between 6 cm and 20 cm at this resolution, and the derived rotation measures, as discussed in the text. The rotation measures shown for the northern lobe are the smallest possible values. There may be a 180° ambiguity in each 20 cm value, which would increase the rotation measures by 83 rad m^{-2}. The tick marks on the border reference the position $18^h02^m45.615^s$, + 11° 01' 14.6" (epoch 1950).

tude. However, there is an unknown efficiency factor in converting this energy into the line emission. If there is $\sim 10^{60}$ erg available for the shock ionization, that would support the line emission (at its observed rate) for $\sim 10^9$ yr. Collisional ionization may thus provide a viable mechanism for explaining the observed properties of the ionized gas.

From our VLA data, we can calculate a *lower limit* of approximately 1 million years for the age of 3C 368, assuming the source is in the plane of the sky, and that the hotspots advance at a speed of approximately 0.1c (Myers and Spangler 1985). On the other hand, our derived characteristics for 3C 368 also show that the source must have recently been active in relativistic particle acceleration. The synchrotron lifetime of the electrons radiating at 5 GHz in the minimum-pressure magnetic field is only 5×10^4 yr (van der Laan and Perola 1969). This short synchrotron lifetime requires that *in situ* particle acceleration occur in the hotspots of 3C 368. At the current radio luminosity, the total energy of the radio source will be radiated in 10^6 yr. This lifetime estimate applied to Cyg A gives 3×10^7 yr. The total radiative lifetime of 10^6 yr suggests that 3C 368 is a relatively young radio source, and the 5×10^4 yr particle lifetimes at 5 GHz require a very recent energy input. This is consistent with our picture, in which a particular recent merger with a gas-rich galaxy provided the trigger and/or the fuel for both the star formation and the radio activity.

An alternative hypothesis is that the gas represents a line-emission superfilament from a massive cooling flow (Fabian *et al.* 1986), in which a massive burst of star formation occurs. We cannot discount this possibility, but in our opinion it seems less likely than the merger hypothesis, and for the following reasons: First of all, we do know that mergers occur, that they were probably more frequent and gas rich in the past (e.g., at the lookback time to 3C 368), and that they can be connected both with enhanced star formation and nuclear activity. We do not know that x-ray clusters of galaxies exist at such large redshifts; what is needed is a well-formed cluster that already managed to produce its x-ray gas and start a cooling flow onto the dominant cluster member. Furthermore, there is no reason why there would be such good positional and morphological correspondence between the stellar continuum and the emission-line gas in 3C 368. Star formation in cooling flows was never observed directly, except, perhaps, in a couple of objects such as NGC 1275, but the star-formation rate in 3C 368, which we infer from our data and population-synthesis models, is orders of magnitude larger than anything known among the low-redshift cooling-flow galaxies. Even in the low-redshift cooling flows, the estimates of mass-infall rates differ by orders of magnitude (cf. Fabian, Nulsen, and Canizares 1982; and Silk *et al.* 1986, for two different views). Finally, the form of

the IMF in star-forming cooling flows is quite controversial, and it was often stated that predominantly low-mass stars would be formed (Sarazin and O'Connel 1983), which would probably fail to match the observed visual (rest-frame UV) brightness of 3C 368. In these circumstances, we believe that the "minimal" hypothesis that can explain 3C 368 without any special adjustments is a gas-rich merger. Observations of this system with a future space-based x-ray facility may detect a hot cluster gas around this source, and if that happens, the cooling-flow hypothesis may regain some interest.

We thus believe that the imaging and spectroscopic data favor the picture of 3C 368 as a strongly dissipative merger of gas-rich galaxies in a high-redshift cluster. This is the very process that supposedly formed (or at least substantially fattened) the present-day cD galaxies, and we are probably witnessing directly the "secondary" formation of a giant elliptical (or a cD) galaxy. The merging is almost certainly triggering lots of star formation, perhaps through the shock-wave compression mechanism, which makes the galaxy as bright and as blue as observed. That conversion of the kinetic energy of infalling and colliding gas clouds into the light emitted by the newly formed stars, and the generous ionization of the large amounts of gas, as evidenced by the enormous strength of the [O II] emission line, suggests that the galaxy merging at large redshifts is a *highly* dissipative process. It is dubious how realistic or how physically complete are the usual applications of dissipationless soft-gravity N-body simulations in modeling such phenomena.

Many authors have proposed that the galaxian nuclear activity and/or the enhanced star formation are induced by interactions or mergers (cf. the reviews by Balick and Heckman 1982; or Stockton 1986, and references therein). An extensive, albeit mostly circumstantial, evidence that interaction and mergers must have been very common for the relatively nearby powerful radio galaxies was published recently by Heckman *et al.* (1986). Merging may provide a fuel for the central engine which powers the radio lobes, but it may also stimulate the star formation in the main body of a galaxy. This picture may apply to all forms of active nuclei, from narrow-emission-line radio galaxies like 3C 368, to quasars (an interesting example of a moderate-redshift QSO embedded in an [O II] emission-line cloud, 3C 275.1, was discussed recently by Hintzen and Romanishin 1986)).

In all scenarios of galaxy and large-scale structure formation, the rate of mergers in the comoving coordinates is a function of time, and thus the redshift, and it will generally decrease as the number of potential "victims" goes down and the galaxies are carried apart in the Hubble flow. However, it must have taken some time for the initial activity triggered by the early mergers to develop, and the number of active galaxies would have originally *increased* with the cosmic epoch. We know that the comoving number density of *all* forms of active galaxies increases with the redshift, and for most of them flattens or even drops after $z \sim 2$–3. In particular, there is a real, observed cutoff of powerful 3C sources at $z \simeq 2$; such a cutoff was also required by the models of radio-source counts (Windhorst 1984). This behavior is qualitatively in agreement with the simple merger picture sketched above, although the real situation is probably vastly more complex. It is intriguing that the same physical process, gas-rich mergers at large redshifts, may have been the cause of both the secondary formation of cD galaxies and the appearance of powerful radio sources at $z \sim 1$–2.

IV. A JET–GALAXY INTERACTION?

There is an intriguing coincidence in that the P.A. of the galaxy and its associated line emission is practically equal to the P.A. of the radio lobe axis, and that the lobe separation is comparable to the optical size of the galaxy. This may be simply a projection effect: out of ~ 20 radio galaxies currently known at $z > 1$, this one good case may be a chance occurrence. On the other hand, a possibility of real physical association of radio lobes' plasma with the line emission cannot be discounted. We observed the 3C 368 system with the VLA in order to distinguish between these two possibilities.

There are many known occurrences of interactions of radio jets with the gaseous material of the parent galaxy at the low redshifts; see, for example, the review by van Breugel (1986), and the references therein. There is one famous case, Minkowski's object (van Breugel *et al.* 1985; Brodie *et al.* 1985), in which a starburst in a gas-rich dwarf galaxy is apparently triggered by the radio jet of a nearby giant elliptical. In this and other cases, line emission is enhanced at the edges of the jet–gas interaction region, and a patchy screen of plasma in that boundary layer depolarizes the radio emission from the lobe or jet. Note that depolarization and the Faraday rotation may be introduced simply by viewing a radio lobe through a region of ionized gas, even without any dynamically significant interaction.

We can examine the data with regard to these two possibilities. Unfortunately, because of the great distance to 3C 368, even the high-resolution A array maps and the best-seeing optical imaging data do not provide an adequate angular resolution of this system, in comparison to the low-redshift objects reviewed by van Breugel (1986). The detection of a radio core allows us to tentatively overlay the radio map with the [O II] image. If we align the radio core with the peak of the [O II] distribution, which is itself also coincident with the peak in the continuum emission, the southern radio lobe coincides with the optical continuum and line emission, whereas the northern lobe lies outside the visible optical image (Fig. 9). This alignment is very tentative, because the relative astrometry uncertainty is comparable to the angular size of the lobes themselves. There is no evidence that the line emission is enhanced at the edges or boundaries of the radio source; instead, at this resolution the [O II] distribution appears center filled, in contrast to the edge-brightened radio structure.

Both lobes of the radio source show Faraday depolarization between 6 and 20 cm wavelengths. This suggests that the radio and optical emission regions are spatially related, and not just coincident in projection.

In the S hotspot, the ratio of 20 to 6 cm fractional polarization is between 0.2 and 0.3. The three wavelength measurements of polarization position angle show a greater than 180° rotation and indicate a rotation measure (RM) of approximately 80 rad m^{-2}. This RM is nearly constant across the region. At higher resolution the south bridge emission, directly behind the 11% polarized hotspot, is less than 3% polarized. At similar linear resolution, nearby 3CR sources typically have bridge polarizations of approximately 30% (Leahy *et al.* 1986). These polarization data indicate that there is probably a significant gradient in the density of thermal material towards the galaxy nucleus.

The situation in the N lobe is less clear. At different locations within the lobe it is depolarized 2 to 3 times more than the S lobe. The higher-resolution 6 cm data resolve the N lobe into two components with different polarization posi-

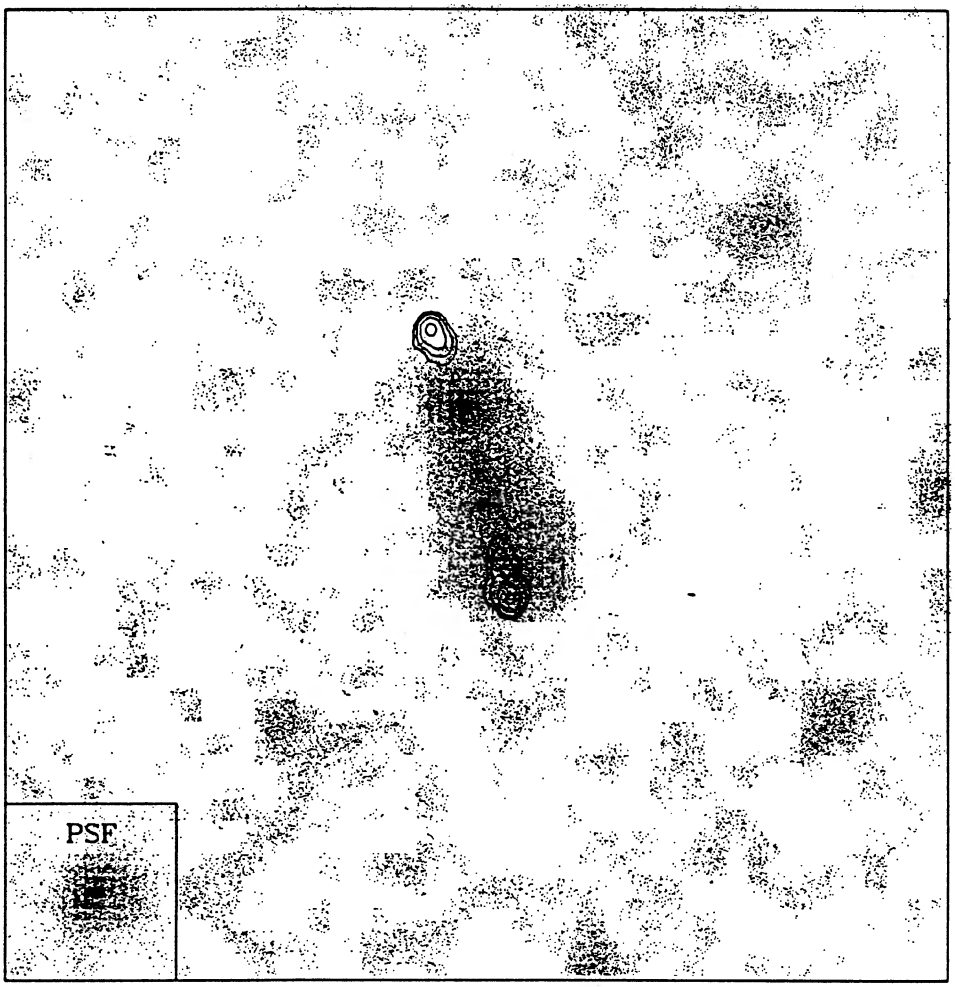

FIG. 9. Repeat of the [O II] image from Fig. 2, with the VLA 6 cm contour map overlaid. It was assumed that the radio core (shown in Fig. 7, but not visible in this map) is coincident with the central peak of the [O II] and optical continuum emission. Note a good positional coincidence, at least in projection, between the southern radio lobe and the emission-line gas.

tion angles, indicating that substantial depolarization may be occurring through averaging within the beam. The polarization position angle shows a large rotation across the region, indicative of a RM change of 25 rad m^{-2}. The present data do not allow us to determine whether an extra 180° of rotation (83 rad m^{-2}) has occurred by 20 cm. Thus, the average rotation measure of approximately 35 rad m^{-2} in the N lobe, as well as the gradient across the lobe, may be considerably larger. The data on both lobes suggest that depolarization occurs through averaging of Faraday rotation measure gradients across the beam. It is currently not possible to determine whether the thermal plasma is in an external screen or mixed with the relativistic plasma.

There may be some evidence that the radio and optical emission regions are dynamically interacting. Recall that the *northern* side of the optical image shows the larger velocity gradient and the velocity width of the [O II] line, and that the velocity width ($\sim$ turbulence) profile (Fig. 6) actually shows a maximum coincident with the "optical N lobe," presumably one of the merging galaxies. However, the northern radio lobe seems to lie outside the optical image, and the kinematical activity of the emission-line gas may be unrelated to the radio source. On the other side, the equivalent width of [O II] is actually larger in the south, where there is a possible overlap of the radio lobe and the optical and line emission. This may be symptomatic of an interaction of the radio lobe (and a jet?) of 3C 368 with its southern gas-rich galaxy component. It is possible, though perhaps less likely, that we are simply seeing the S lobe behind the gas ionized by the collision shock. We cannot tell whether any of the *star formation* is enhanced by this tentative jet–galaxy interaction. There is no significant difference in the observed *BVR* colors between the northern and the southern optical "lobes" of the galaxy.

Another possibility is that the gas has been entrained into, and accelerated by, the radio plasma, similar to what seems to be occurring in the lower-luminosity radio source 4C 29.30 (van Breugel *et al.* 1986), where an Hα filament is accelerated by a nearby radio jet. We do not have sufficient resolution to follow this possibility further. The above evidence does not present a clear case for a dynamical interaction between the radio and thermal plasmas.

V. CONCLUSIONS

We have shown that the observed properties of 3C 368 can be understood as a spectacular dissipative merger at a high redshift: the process of accretion of smaller, gas-rich galaxies, accompanied with the vigorous star formation, is almost a replay of the dissipative processes that may have occurred

during the epoch of "primary" galaxy formation (Silk and Norman 1981). In this picture, the star formation in 3C 368 is induced by the shock compression of the gas in merging galaxies, which now play the role of protogalactic fragments in the Silk-Norman model. Substantial amounts of kinetic energy may be reradiated as a consequence of induced star formation. The merger is indicated by the shape of the optical continuum and [O II] images, and the general properties of extended emission-line gas. The evidence for enhanced star formation is provided by the high luminosity and blue colors of the galaxy's stellar continuum. If we assume that the star formation in 3C 368 is roughly described by the $\mu = 0.5$ Bruzual model at the age of 3 Gyr, and use the observed visual magnitude for scaling, we derive the star-formation rate of about $350\,\mathcal{M}_\odot\ \mathrm{yr}^{-1}$, comparable to the most spectacular starbursts known at the low redshifts. In other words, we are probably witnessing the dynamical, "secondary" formation of a large elliptical, or perhaps a cD galaxy at a lookback time of $\sim 2/3$ of the present galaxian age. Of course, we do not know how much of the kinetic energy of the merging galaxies will be simply distributed among the stars, nor exactly what the end product of this merger will look like (a cD galaxy, or something else).

Some, but possibly not much, of the extended line emission may be due to an interaction between the southern radio lobe or jet with a gas-rich galaxy component; the evidence for such interaction is ambiguous. Even the occurrence of a possible interaction between the radio lobes and the ambient gas does not preclude the interpretation of this system as a merger. In practically all cases of radio galaxies with tentative interactions between the radio plasma and the ambient gas that were investigated by van Breugel, Heckman, and their colleagues, there are morphological indications suggestive of recent mergers (tidal tails, shells, etc.). An ongoing gas-rich merger may simply provide the suitable environment for such interaction to occur, as well as the fuel for the central engine which generates the radio jets in the first place.

The morphology of 3C 368 is not unique: many of the $z > 1$, 3CR radio galaxies have elongated, asymmetric, or even multimodal shapes, and have a strong [O II] line emission associated with them. It is quite possible that all of them are still relatively young and growing giant ellipticals, vigorously merging with their smaller, gas-rich companions. The mergers may be the source of fuel for the central engine that builds the powerful radio lobes, and may also be the immediate cause of enhanced star formation in these distant galaxies, which is necessary to explain their large luminosities and blue colors. This has immediate implications for the studies of galaxy evolution that use the radio-selected samples: The evolution models favored by the colors and magnitudes of the 3CR radio galaxy sample are those with a continuing, but ever declining star formation; e.g., the Bruzual μ models (cf. Djorgovski, Spinrad, and Dickinson 1987; or Djorgovski, Spinrad, and Marr 1985). These models may now be understood as a sequence of starbursts, perhaps triggered by the mergers, declining exponentially in time in intensity and/or rate, rather than a smoothly decaying star formation in an isolated galaxy (NB: the Bruzual models in their simplest form, used by most authors, do not include an infall of any fresh material). This interpretation is close to the one proposed by Lilly and Longair (1984), in which a passively evolving giant elliptical (with a bulk of the stars created in the initial burst) undergoes "rejuvenating" starbursts which make the magnitudes brighter and the colors bluer. Such processes may even provide a physical explanation for a tentative correlation between the radio power and the near-IR luminosity, as proposed by Yates *et al.* (1986). Note, however, that this interpretation requires a very good correlation between the intensity of a starburst and the power pumped in the radio lobes, as well as a rapid turnaround in the central engine.

We wish to thank the crews of several observatories, who helped in obtaining the data used here: Kitt Peak, CFHT, VLA, and Lick. S. D. was supported in part by Harvard University. H. S. was supported by the NSF grant AST85-13416. L. R. and J. P. were supported by NSF grants AST83-15949 and AST84-05930. A. S. was supported by NSF grant AST83-17457. S. D. and H. S. would like to thank the Canadian CFHT time-allocation committee for the observing time during which some of the data presented here were obtained.

REFERENCES

Baade, W., and Minkowski, R. (1954a). Astrophys. J. **119**, 206.
Baade, W., and Minkowski, R. (1954b). Astrophys. J. **119**, 215.
Balick, B., and Heckman, T. (1982). Annu. Rev. Astron. Astrophys. **20**, 431.
Brodie, J., Bowyer, S., and McCarthy, P. (1985), Astrophys. J. Lett. **293**, L59.
Bruzual, G. (1981). Ph. D. thesis, University of California, Berkeley.
Bruzual, G. (1983). Astrophys. J. **273**, 105.
Burns, J. O., Owen, F.N., and Rudnick, L. (1979). Astron. J. **84**, 1683.
Burstein, D., and Heiles, C. (1982). Astron. J. **87**, 1165.
Christian, C., Adams, M., Barnes, J., Butcher, H., Hayes, D., Mould, J., and Siegel, M. (1985). Publ. Astron. Soc. Pac. **97**, 363.
Djorgovski, S. (1987). In *Nearly Normal Galaxies: From Planck Time to the Present*, Proceedings of the Santa Cruz Workshop, edited by S. Faber(Springer, Berlin) (in press).
Djorgovski, S., Spinrad, H., and Dickinson, M. (1987). Astrophys. J. (submitted).
Djorgovski, S., Spinrad, H., and Marr, J. (1985). Lect. Not. Phys. **232**, 193.
Fabian, A., Arnaud, K., Nulsen, P., and Mushotzky, R. (1986). Astrophys. J. **305**, 9.
Fabian, A., Nulsen, P., and Canizares, C. (1984). Nature **310**, 733.
Fanaroff, B., and Riley, J. (1974). Mon. Not. R. Astron. Soc. **167**, 31p.
Gunn, J., Hoessel, J., Westphal, J., Perryman, M., and Longair, M. (1981). Mon. Not. R. Astron. Soc. **194**, 111.
Heckman, T., Smith, E., Baum, S., van Breugel, W., Miley, G., Illingworth, G., Bothun, G., and Balick, B. (1987). Astrophys. J. **311**, 526.
Hintzen, P., and Romanishin, W. (1986). Astrophys. J. Lett. **311**, Ll.
Kellermann, K.I., Pauliny-Toth, I.I.K., and Williams, P. J. S. (1969). Astrophys. J. **157**, 1.
Leahy, J., Pooley, G., and Riley, J. (1986). Mon. Not. R. Astron. Soc. **222**, 753.
Lebofsky, M., and Eisenhardt, P. (1986). Astrophys. J. **300**, 151.
Lilly, S., and Longair, M. (1984). Mon. Not. R. Astron. Soc. **211**, 833.
Myers, S.T., and Spangler, S.R. (1985). Astrophys. J. **291**, 52.
Perley, R.A., Dreher, J.W., and Cowen, J.J. (1984). Astrophys. J. Lett. **285**, L35.
Sarazin, C., and O'Connel, R. (1983). Astrophys. J. **268**, 557.
Silk, J., Djorgovski, S., Wyse, R., and Bruzual, G. (1986). Astrophys. J. **307**, 415.
Silk, J., and Norman, C. (1981). Astrophys. J. **247**, 59.

Spinrad, H. (1986). Publ. Astron. Soc. Pac. **98**, 269.
Spinrad, H., and Djorgovski, S. (1984a). Astrophys. J. Lett. **280**, L9.
Spinrad, H., and Djorgovski, S. (1984b). Astrophys. J. Lett. **285**, L49.
Spinrad, H., and Djorgovski, S. (1987). In *Observational Cosmology*, IAU Symposium No. 124, edited by G. Burbidge (Reidel, Dordrecht) (in press).
Spinrad, H., Djorgovski, S., Marr, J., and Aguilar, L. (1985). Publ. Astron. Soc. Pac. **97**, 932.
Stockton, A. (1986). Astrophys. Space Sci. **118**, 487.
Stone, R. (1977). Astrophys. J. **218**, 767.
van Breugel, W. (1986). Can. J. Phys. **64**, 392.
van Breugel, W., Filippenko, A., Heckman, T., and Miley, G. (1985). Astrophys. J. **293**, 83.
van Breugel, W., Heckman, T., Miley, G., and Filippenko, A. (1986). Astrophys. J. **311**, 58.
van der Laan, H., and Perola, G.C. (1969). Astron. Astrophys. **3**, 468.
Windhorst, R. (1984). Ph. D. thesis, University of Leiden.
Yates, M., Miller, L., and Peacock, J. (1986). Mon. Not. R. Astron. Soc. **221**, 311.